Summary Report on Work Performed by the U.S. Home Team in the Blanket Design Task D307A, Subtask 1.2

Nuclear Analysis in Support of Blanket and Vacuum Vessel Design

M.E. Sawan and H.Y. Khater

March 1997

UWFDM-1043

Also ITER/US/97/IV-BL-4.

FUSION TECHNOLOGY INSTITUTE

UNIVERSITY OF WISCONSIN

MADISON WISCONSIN

ITER/US/97/IV-BL-4

Summary Report on Work Performed by the U.S. Home Team in the Blanket Design Task D307A, Subtask 1.2

Nuclear Analysis in Support of Blanket and Vacuum Vessel Design

Mohamed E. Sawan and Hesham Y. Khater

Fusion Technology Institute
Department of Nuclear Engineering and Engineering Physics
University of Wisconsin-Madison
1500 Engineering Drive
Madison, WI 53706

March 1997

UWFDM-1043

Executive Summary

During the year 1996, the U.S. home team performed neutronics and activation analyses as part of the blanket design task D307. The design of ITER has been evolving during the EDA phase. A major part of this task involved modeling the detailed geometrical configuration of the Interim ITER Design for 3-D neutronics calculations. The divertor cassette model was completed for MCNP calculations. The model represents a nine degree toroidal sector of ITER. Hence, it includes one and a half cassettes with the associated gaps. The model includes separate regions for the outer leg, inner leg, wings, dome, lining, and pumping ducts. Each region is divided into many cells to allow determination of the detailed spatial variation of nuclear parameters in the cassette.

The 3-D divertor cassette model has been integrated with the general ITER model. The integrated model includes detailed modeling of the first wall, blanket with associated coolant manifolds and back plates, VV, TF coils, central solenoid, and PF coils. All toroidal and poloidal gaps between adjacent blanket modules are included. The major vacuum vessel penetrations are included in the model. This includes the divertor port at the bottom of the reactor. No additional shielding is included around the port. The TF coils are segmented to determine the nuclear heating and damage in the parts adjacent to the port resulting from radiation streaming. The neutronics parameters have been calculated in the different components of the divertor cassette. These parameters included nuclear heating, atomic displacement and helium production.

Radiation damage to parts of the vacuum vessel in the divertor region have been quantified to assess the feasibility of rewelding. The peak helium production value of about 0.5 He appm/FPY indicates that rewelding of parts of the VV behind the pumping ducts at the bottom of cassettes might be feasible. Since these areas of relatively high helium production are very small, the design of the VV can locate the welds away from streaming paths if these values are of concern for rewelding. The largest damage in the divertor port occurs at the location where the port wall joins to the front VV wall. The peak helium production is 0.036 appm/FPY indicating that rewelding of the divertor port is feasible.

The peak magnet radiation effects have been calculated in segments of the TF coils in the divertor region. The radiation effects are higher at the side surface due to the effect of streaming. The calculated radiation effects are much lower than the radiation limits considered in ITER. The total nuclear heating in the parts of the 20 TF coils in the divertor region is 2.08 kW with 1.58 kW contributed by the parts adjacent to the divertor port. It is essential to determine the additional heating in the other parts of the coils and add them to the contribution from the divertor region to determine whether the total heating limit of 17 kW can be satisfied.

We started modifying the 3-D model to include more details and design modifications in the divertor cassette based on the ITER Detailed Design. Our effort concentrated on implementing the changes in the divertor cassette design that have been nearly fully developed. Separate regions are included to represent the mechanical attachments and coolant pipe connections for the dome, vertical targets, and wings. The layered configurations of the dome PFC and vertical targets were modeled accurately with the front tungsten layer modeled separately. The heterogeneous model used will accurately account for the self-shielding effect of the giant resonance at 20 eV that produces W-187. The geometrical model for MCNP has been developed and tested by spraying it with 20 million particles. We will start implementing modifications in the blanket design when the design becomes fully developed. Discussions have started with the Nuclear Analysis group in Garching to identify the modifications needed.

A new processed multigroup library based on FENDL-1 has been provided. The library includes gas production cross sections and decay energy. The beta decay energy is assumed to be deposited locally and is added to the neutron kerma while the gamma production cross sections are modified to include the produced decay gamma thus allowing them to be transported before depositing their energy. This is a better treatment for decay gamma than assuming that all energy is deposited locally. We used the TRANSX code to generate updated working multigroup cross section libraries with two different group structures.

The activation code DKR-PULSAR1.0 and its associated data libraries have been modified to allow for improved activation analysis. We expanded the DKR-PULSAR1.0 code capabilities to allow for 3-D activation calculations. The activation cross section library was updated to include the latest cross section data from FENDL1.0. We updated the DKR-PULSAR1.0 gamma source data according to the latest ENDF/B-VI values. Activation calculations have been performed under this task agreement in support of the ITER building dose calculation. The gamma source from radioactive nuclide decay was determined for all mesh points after shutdown for dose calculations.

1. Introduction

During the year 1996, the U.S. home team performed design tasks in the neutronics and activation area as part of the blanket design D307. These included responding to specific requests by the Nuclear Analysis group in Garching. A major part of the work performed involved detailed three-dimensional modeling of the ITER reactor based on the Interim Design. Three-dimensional neutronics calculations have been carried out to determine the nuclear parameters (nuclear heating, atomic displacement, and gas production) in the divertor cassette. In addition, radiation damage to parts of the vacuum vessel in the divertor region have been quantified to assess the feasibility of rewelding. This is of particular interest for parts of the vacuum vessel exposed to neutrons streaming through the divertor pumping ducts and the large divertor ports. The peak magnet radiation effects have been calculated in segments of the TF coils in the divertor region to assess the impact of streaming through the divertor ports on peak local magnet radiation effects and total nuclear heating. In the last quarter of 1996, we started modifying the 3-D model to include more details and design modifications in the divertor cassette based on the ITER Detailed Design. Furthermore, we processed the most recent multigroup FENDL library that includes gas production and decay energy to generate multigroup working libraries. Several activities have been performed under this task in support of the ITER building dose calculation. These involved updating the activation code DKR-PULSAR1.0 and its libraries, and performing multi-dimensional activation calculations to determine the decay gamma resulting from activation of the building. This report summarizes the neutronics and activation tasks performed during the year 1996 as part of the blanket design task D307.

2. Three-Dimensional Neutronics and Shielding Analyses for the Divertor Region

The divertor cassette design went through several changes to improve its performance. Neutronics and shielding features were considered for the design variations. The Interim ITER design utilizes 60 divertor cassettes with vertical targets and a central dome [1]. Knowledge of nuclear heating and radiation damage levels in the different components of the divertor cassette is essential for proper design analysis. Twenty large divertor ports are utilized for assembly and disassembly of the divertor cassettes and for vacuum pumping. Radiation streaming into these ports can produce excessive heating and damage in the TF coils in the divertor region. Reducing nuclear heating and radiation damage in the TF coils to acceptable levels particularly in the regions behind the divertor cassettes and adjacent to the large divertor ports is an important shielding issue. Radiation damage to parts of the vacuum vessel (VV) in the divertor region need to be quantified to assess the feasibility of rewelding. Due to the geometrical complexity of the divertor region, three-dimensional (3-D) analyses are required.

2.1. Three-Dimensional Calculational Model

Due to the geometrical complexity of the divertor region, 3-D models are required to properly determine the nuclear parameters. 3-D neutron-gamma transport calculations have been performed for the divertor region. The continuous energy, coupled neutron-gamma-ray Monte Carlo code MCNP-4A [2] has been used. The nuclear data used is based on the most recent FENDL-1 evaluation [3]. A recent version of the ACE files was provided by R. E. MacFarlane of Los Alamos National Laboratory. This version includes gas production cross sections and damage energy cross sections which are important design relevant parameters. Reaction number 444 is used in tally multipliers to calculate atomic displacements. We used this recent version of the library to perform the detailed three-dimensional neutronics and shielding calculations for the ITER reactor. Using the FENDL cross section library revealed problems associated with some of the elements in the library. Adding gas production and damage data to the processed library is very helpful and convenient for calculating design relevant parameters. However, gas production and damage data are not included for carbon. The file for Na-23 from JENDL 3.1 has not been updated and presumably does not include gas production and damage data. ENDF/B-VI files are provided for He-3, He-4, Sc-45, and Au-197 which are not in the FENDL/E-1.0 material list. Data for helium have been used in the ITER calculation where liquid He is used in the magnets. The BROND-2 files for H-2 and N-14 did not work with MCNP. The ENDF/B-VI files were substituted for these isotopes. These problems were brought to the attention of the group at LANL working on generating the FENDL library for MCNP.

The detailed geometrical configuration of the divertor cassette has been modeled for 3-D neutronics calculations. The drawings provided by the Joint Central Team (JCT) at Garching for the interim ITER design are the basis for the 3-D modeling. The model represents a nine degree toroidal sector of ITER. Hence, it includes one and a half cassettes with the associated 1 cm gaps between adjacent cassettes. The model includes in detail the high heat flux plasma facing components (PFC), the vertical targets, the wings with associated plates, the gas boxes, as well as the central dome and cassette bodies. The 37.5 cm wide and 17.5 cm thick divertor pumping duct at the bottom of each cassette is included in the model. The rails upon which the cassettes move toroidally during maintenance are also included. The cassette model is divided into 32 cells to allow determination of the detailed spatial variation of nuclear parameters in the cassette. Figure 1 shows a vertical cross section of the cassette model at a toroidal location at the center of the cassette through the pumping ducts.

The divertor cassette model has been integrated with the general ITER model. The integrated model includes detailed modeling of the first wall, blanket with associated coolant manifolds and back plates, VV, TF coils, central solenoid, and PF coils. All toroidal and poloidal gaps between adjacent blanket modules are included. The major vacuum vessel penetrations are included in the model. This includes the divertor port at the bottom of the reactor. Due to symmetry, only 1/40 of the reactor is modeled with surrounding reflecting boundaries. The model includes half a TF coil and half a divertor port. The divertor port is 254.5 cm high with a width increasing from 97 cm at the bottom to 176 cm at the top. The port wall is

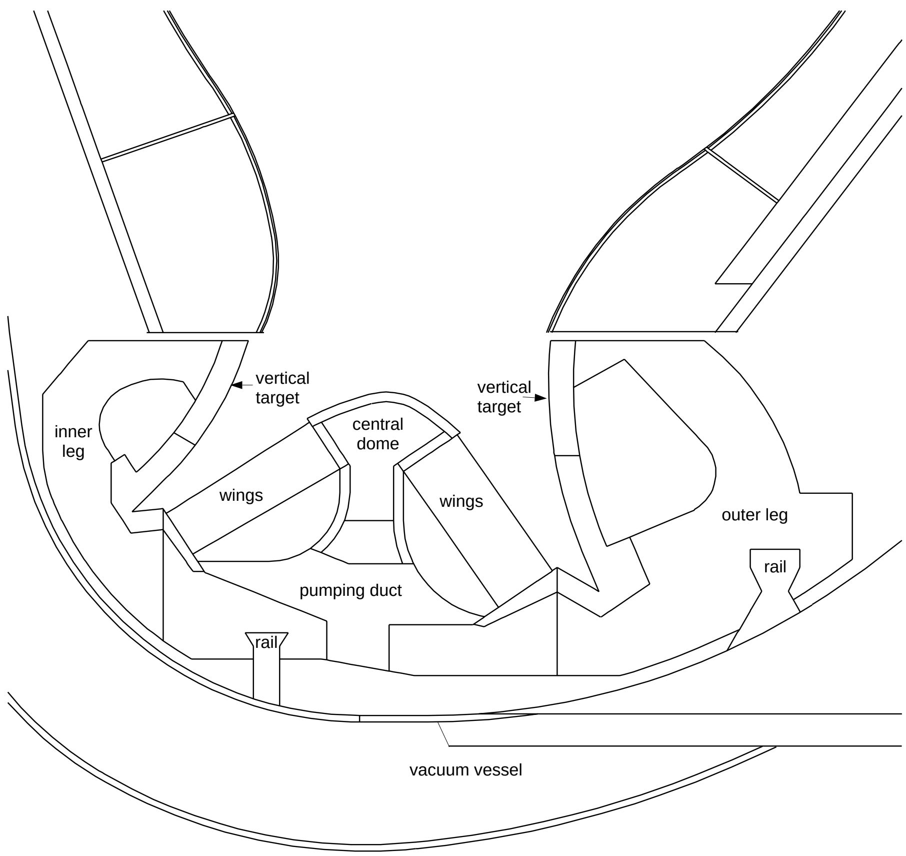

Fig. 1. Vertical cross section at the middle of the cassette model.

20 cm thick and is assumed to consist of 80% 316SS and 20% water. No additional shielding is included around the port. The TF coils are segmented to determine the nuclear heating and damage in the parts adjacent to the port resulting from radiation streaming.

The output of the MCNP geometry plotting routine given in Fig. 2 shows vertical cross sections through the middle of the vacuum vessel ports. The detailed reactor geometrical modeling is illustrated. Figure 3 is a horizontal cross section at z= -6 m in the middle of the divertor port. The divertor pumping ducts in the divertor cassettes are shown in this figure. Also shown is the part of the TF coil adjacent to the divertor port. A coil case which is about 20 cm thick surrounds the winding pack. Several additional surfaces have been added in the divertor region to allow for utilizing the geometry splitting with the Russian Roulette variance reduction techniques employed in MCNP, needed to improve the accuracy of the calculated nuclear responses.

A combination of cones, tori, cylinders, and planes was utilized for accurate modeling of the geometry. A total of 475 surfaces has been used in the model, of which 164 are fourth degree tori. The model employs 417 geometrical cells. The volumes of the different cells and the areas of surfaces of interest have been determined stochastically by ray tracing. In this calculation, all cells are assumed to not include any material and the geometrical model has been sprayed by 10 million particles at random directions. This calculation serves also as a means for geometry checking by making sure that each point in space belongs to one of the cells used in the model. This calculation provided a successful check for the geometrical model.

A source subroutine has been written to modify MCNP to sample source neutrons from the source distribution in the ITER plasma provided numerically by the San Diego JCT at 1600 mesh points. Surface flux tallies are used to determine the peak radiation effects at the front surfaces of the different components of the divertor cassette, VV and TF coil and cell flux and energy deposition tallies are used to determine the volume averaged parameters and total nuclear heating in the components of the divertor and TF coil. The appropriate material compositions are used for the different cells of the model. The VV consists of two 4 cm thick 316SS plates

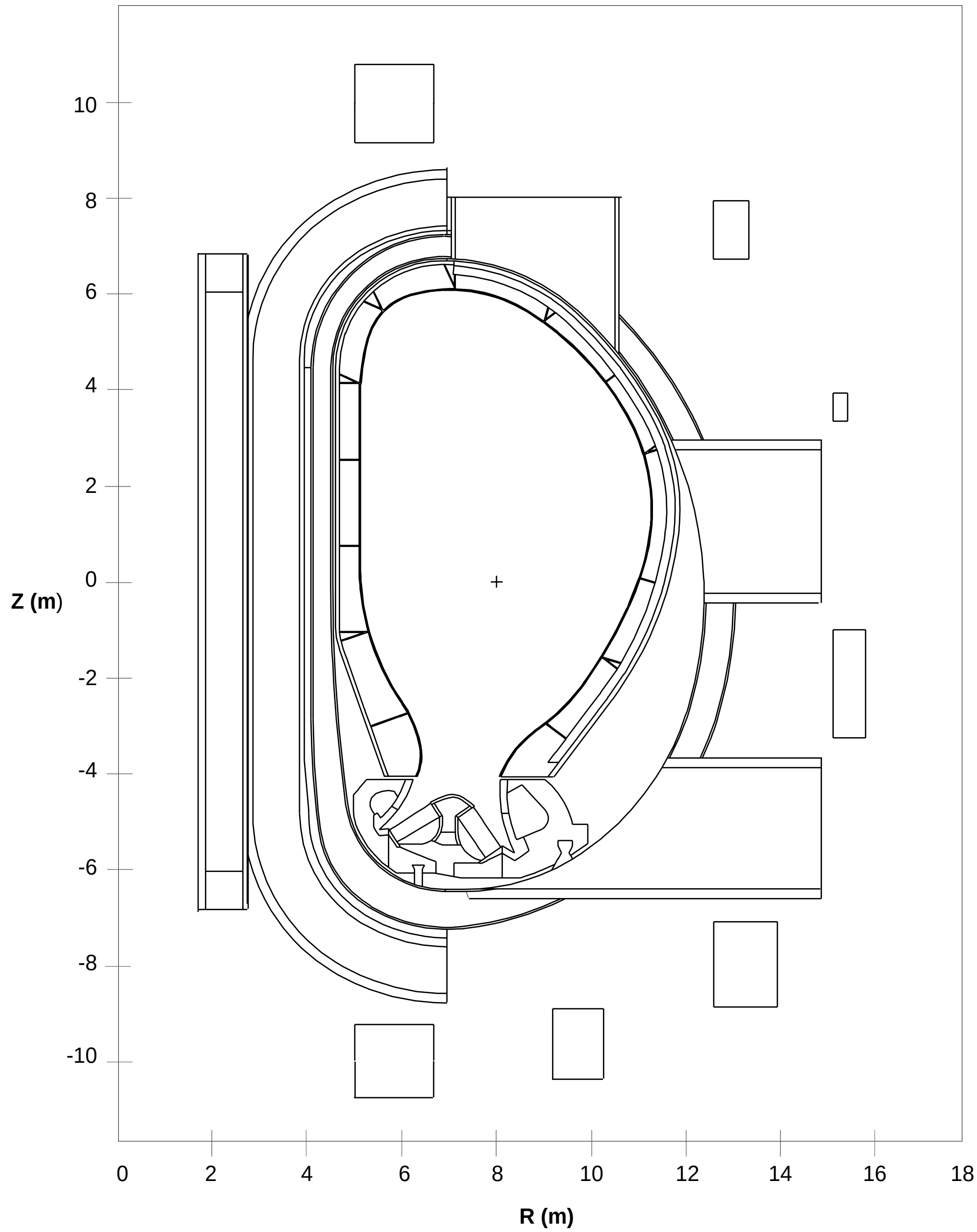

Fig. 2. Vertical cross section through the VV ports of the ITER 3-D model for MCNP calculations.

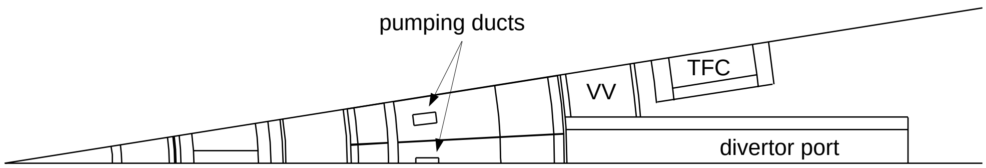

Fig. 3. Horizontal cross section of the 3-D model at Z= -6 m.

sandwiching a shielding region made of 60% 316SS and 40% water. The winding pack of the TF coil consists of 43.2% SS, 11.7% Cu, 2.9% Nb_3Sn, 7.4% Bronze, 16.8% liquid He, and 18% insulator (epoxy with 70% R-glass). The material composition used for the divertor cassette is given in Table 1. The calculation has been performed using 100,000 source particles yielding statistical uncertainties less than 10% in the calculated nuclear responses at the locations of interest. The calculation used 32 hours of CPU time on the Cray-2. The results are normalized to the nominal fusion power of 1500 MW. The end of life fluence related radiation effects have been determined for 1 full power year (FPY) of operation.

Table 1. Material Composition

Dome PFC	14% W, 13% Cu, 29% SS, 44% water	
Central Dome Body	80% SS, 20% water	
Wings	16% W, 79% Cu, 5% water	
	packing fraction: 21% outer, 26% inner	
Gas Box Liners	8% W, 74% Cu, 18% water	
Vertical Targets	top section:	7% W, 22% Cu, 52% SS, 19% water
	lower section:	17% C, 20% Cu, 46% SS, 17% water
Inner and Outer Legs	80% SS, 20% water	
Rails	100% SS	

2.2. Nuclear Parameters in the Divertor Cassette

The neutronics parameters have been calculated in the different components of the divertor cassette. These parameters included nuclear heating, atomic displacement and helium production. The radiation damage was calculated for both stainless steel and copper structures. The volume averaged parameters were determined for 32 segments of the cassette using cell flux and energy deposition tallies. The peak nuclear responses were determined also at the front surfaces of the cassette components using surface flux tallies. These are given in Table 2. The largest heating and damage occurs in the dome PFC which has a full view of the plasma and has the largest neutron wall loading. The vertical targets and wings experience moderate levels of heating and damage with these values dropping rapidly as one moves deeper in the cassette body. For example, nuclear heating in the outer rail is only 2.9×10^{-4} W/cm^3 and the dpa and helium production values are 6.3×10^{-5} dpa/FPY and 1.3×10^{-3} He appm/FPY. In general, the nuclear parameters in the inboard side of the cassette are lower than those in the outboard side that has a larger view of the plasma. Atomic displacements in Cu are slightly higher than in SS while helium production is much lower because of the higher gas threshold energy of nuclear reactions producing helium. The total nuclear heating has been calculated for the 60 divertor cassettes to be 102.4 MW. The major contributors are the outer vertical target with 23.1 MW and the dome PFC with 19.7 MW.

Table 2. Peak Nuclear Responses in the Divertor Cassette

	Power Density (W/cm^3)	dpa (dpa/FPY)	He Production (appm/FPY)
Dome PFC	10.75	4.69 SS 5.04 Cu	89.16 SS 55.39 Cu
Central Dome Body	5.39	2.28 SS	40.22 SS
Outer Wings	7.34	2.98 Cu	31.26 Cu
Inner Wings	5.79	2.17 Cu	20.40 Cu
Outer Vertical Target	5.46	2.60 SS 2.77 Cu	46.54 SS 26.29 Cu
Inner Vertical Target	3.72	0.95 SS 0.98 Cu	18.31 SS 11.95 Cu

2.3. Nuclear Parameters in Vacuum Vessel

Streaming through the pumping ducts in the bottom of the cassette can result in damage hot spots in the VV behind it. The impact of neutron streaming through the ducts was analyzed for previous designs and recommendations regarding their configuration and size were made to minimize nuclear heating and helium production in parts of the VV behind them. In the Interim Design considered here, the pumping ducts are more inclined towards the outer and inner divertor legs such that the VV behind them does not see any direct neutrons from the plasma.

This helps cut down the He production which is critical for rewelding. Only low energy secondary neutrons stream through the pumping ducts. The VV results were determined both for toroidal locations away from the ducts and behind the ducts by segmenting the front surface of the VV below the cassette. The results are given in Table 3. A peaking factor of about 5 results from streaming through the ducts. The peak helium production value of about 0.5 He appm/FPY indicates that rewelding of parts of the VV behind the pumping ducts might be feasible. Since these areas of relatively high helium production are very small, the design of the VV can locate the welds away from streaming path if these values are of concern for rewelding. Another area of concern for rewelding is the divertor port where relatively high damage is expected due to neutron streaming. The helium production was calculated along the divertor port. The largest damage occurs at the location where the port wall joins to the front VV wall and drops as one moves along the port away from the plasma chamber. The peak helium production is 0.036 appm/FPY and drops to 0.005 appm/FPY at locations adjacent to the back of the TF coil. It is clear from these results that rewelding of the divertor port is feasible.

Table 3. Peak Nuclear Responses in the VV behind the Divertor Cassette

	Power Density (W/cm^3)	dpa (dpa/FPY)	He Production (appm/FPY)
Behind pumping duct	0.034	0.025	0.48
Behind cassette body	0.018	0.005	0.09

2.4. Magnet Radiation Effects in the Divertor Region

The peak magnet radiation effects have been calculated in segments of the TF coils adjacent to the divertor port, between the divertor port and the horizontal port, and behind the divertor cassette below the divertor port. The radiation effects at the front surface of the TF coils adjacent to the divertor port are about an order of magnitude higher than those above and below the port due to radiation streaming through the port as illustrated by the results in Table 4. Table 5 gives the magnet radiation effects in the part of the TF coil adjacent to the divertor port. The results are given at the front and side surfaces of the coil. The radiation effects are higher at

Table 4. Magnet Radiation Effects at Front Surface of the TF Coils in the Divertor Region

	Above Divertor Port	Adjacent to Divertor Port	Below Divertor Port
Coil case power density (kW/m^3)	6.87×10^{-3}	0.080	7.62×10^{-3}
Winding pack power density (kW/m^3)	3.01×10^{-4}	5.12×10^{-3}	3.80×10^{-4}
Insulator dose (Rad/FPY)	4.18×10^{5}	4.46×10^{6}	3.64×10^{5}
Fast neutron fluence (n/cm^2 per FPY)	4.98×10^{14}	6.27×10^{15}	5.28×10^{15}
Copper dpa (dpa/FPY)	3.11×10^{-7}	2.38×10^{-6}	2.29×10^{-7}

Table 5. Magnet Radiation Effects at Front and Side Surfaces of the TF Coils Adjacent to the Divertor Port

	Front surface	Side surface
Coil case power density (kW/m^3)	0.080	0.126
Winding pack power density (kW/m^3)	5.12×10^{-3}	6.38×10^{-3}
Insulator dose (Rad/FPY)	4.46×10^{6}	6.78×10^{6}
Fast neutron fluence (n/cm^2 per FPY)	6.27×10^{15}	1.10×10^{16}
Copper dpa (dpa/FPY)	2.38×10^{-6}	4.46×10^{-6}

the side surface due to the effect of streaming. The calculated radiation effects are much lower than the radiation limits considered in ITER. These radiation limits are 2 and 1 kW/m^3 for the coil case and winding pack power density, respectively, and 1×10^{9} rads for the end-of-life insulator dose [4]. Although no limits were specified for fast neutron fluence and Cu dpa in the EDA, the results are about three orders of magnitude lower than the limits of 1×10^{19} n/cm^2 and 6×10^{-3} dpa used in the CDA [5]. It is clear that the sides of the TF coils are well protected from radiation streaming into the divertor ports.

The total nuclear heating in the parts of the 20 TF coils in the divertor region is given in Table 6. The results are given for the front, back, and side coil cases as well as the winding pack. The total nuclear heating is 2.081 kW with 1.575 kW contributed by the parts adjacent to the divertor port. The statistical uncertainty is less than 5%. The heating in the part below the port is about a factor of 5 more than that in the part above the port. Only 0.03 kW is contributed by the inboard parts of the TF coils behind the divertor cassette. The total nuclear heating in the TF

Table 6. Total Nuclear Heating (kW) in the TF Coils in the Divertor Region

	Above Divertor Port	Adjacent to Divertor Port	Below Divertor Port
Inner case	0.031	0.409	0.036
Outer case	0.005	0.114	0.075
Side case	0.035	0.868	0.249
Winding pack	0.009	0.185	0.065
Total	0.080	1.576	0.425

coils should not exceed 17 kW. It is essential to determine the additional heating in the other parts of the coils and add them to the contribution from the divertor region to determine whether the total heating limit can be satisfied.

It is interesting to note that the results in the winding pack are lower than those in the outline design [6] where additional shielding was provided by the 11 cm support structure between the divertor port and the TF coil. This is attributed partly to the added attenuation in the 20 cm coil case that was not used in the outline design. Furthermore, the present interim design has a thicker outer divertor leg of 48 to 100 cm in addition to the 15 cm thick vertical target compared to a total thickness of only 45 cm in the previous outline design. Also the baffle on the outboard side is more than 1 m thick compared to an 80 cm thick blanket in the previous design. In addition, the pumping ducts in the cassette are pointing downward while they were in the outer leg and pointing directly towards the port in the previous design. These differences result in less streaming into the port and compensate for the loss of the additional 11 cm shielding taken credit for in the previous design.

3. Modification of 3-D Model Based on the ITER Detailed Design

The three-dimensional neutronics model used in the calculations is based on the ITER Interim Design. Modifications to the model has started. The purpose is to include more details and recent design changes implemented in the ITER Detailed Design. Our effort concentrated on implementing the changes in the divertor cassette design that has been nearly fully developed. Each divertor cassette in the model was divided into 103 regions to provide detailed spatial distribution of nuclear heating and radiation damage. The number of regions in the present model is three times that in the previous model. Separate regions are included to represent the mechanical attachments and coolant pipe connections for the dome, vertical targets, and wings. Geometrical changes in the cassette design were also included in the model. The layered configurations of the dome PFC and vertical targets were modeled accurately with the front tungsten layer modeled separately. This was necessary to help resolve the inconsistency in values of the decay heat in tungsten calculated by the JCT and other home teams. It has been shown from one-dimensional calculations that the homogenization of tungsten with steel, copper, and water in the armor and substrates of the PFC can lead to up to a factor of three overestimation (depending on the water content) of the production of the W-187 isotope that dominates the decay heat. The heterogeneous model used will accurately account for the self-shielding effect of the giant resonance at 20 eV that produces W-187. The geometrical model for MCNP has been developed and tested by spraying it with 20 million particles. This also allowed calculation of the volumes and areas of the cassette regions stochastically to be used in the calculation of the nuclear parameters. Figure 4 gives a vertical cross section in the modified ITER model that includes design changes and more detailed segmentation for the divertor cassette. Figure 5 shows the detailed model for the divertor cassette. Discussions are underway with the divertor group of the JCT to define the material compositions to be used in the different regions of the divertor cassette.

We will start implementing modifications in the blanket design when the design becomes fully developed. Discussions have started with the Nuclear Analysis group in Garching to identify the modifications needed. These include the addition of the flexible supports between the outboard blanket and vacuum vessel below the mid-plane port. A boron carbide shield should also be added below the flexible support to assess its impact on magnet heating. The gas seal between the blanket back plate and the vacuum vessel will also be added immediately above the divertor. Since most of the design changes in the blanket are expected to be in the back plate and manifolds, the impact will be mainly on shielding and the impact on nuclear parameters in the divertor cassette will be minimal.

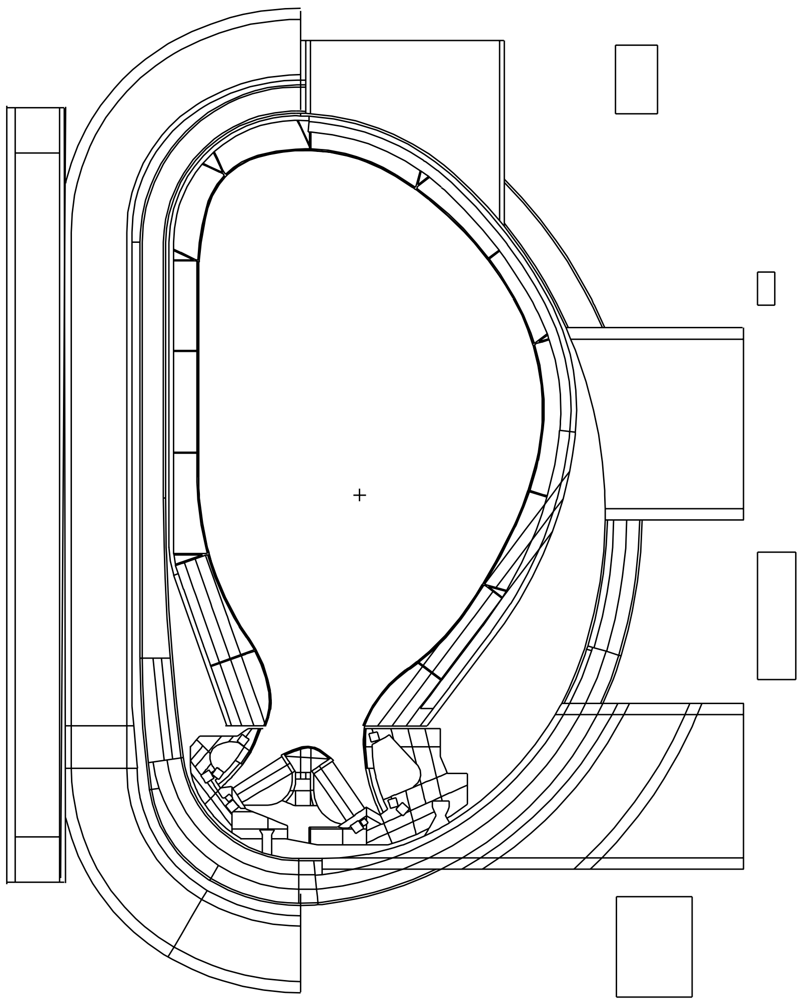

Fig. 4. Vertical cross section through the VV ports of the ITER 3-D model for MCNP calculations.

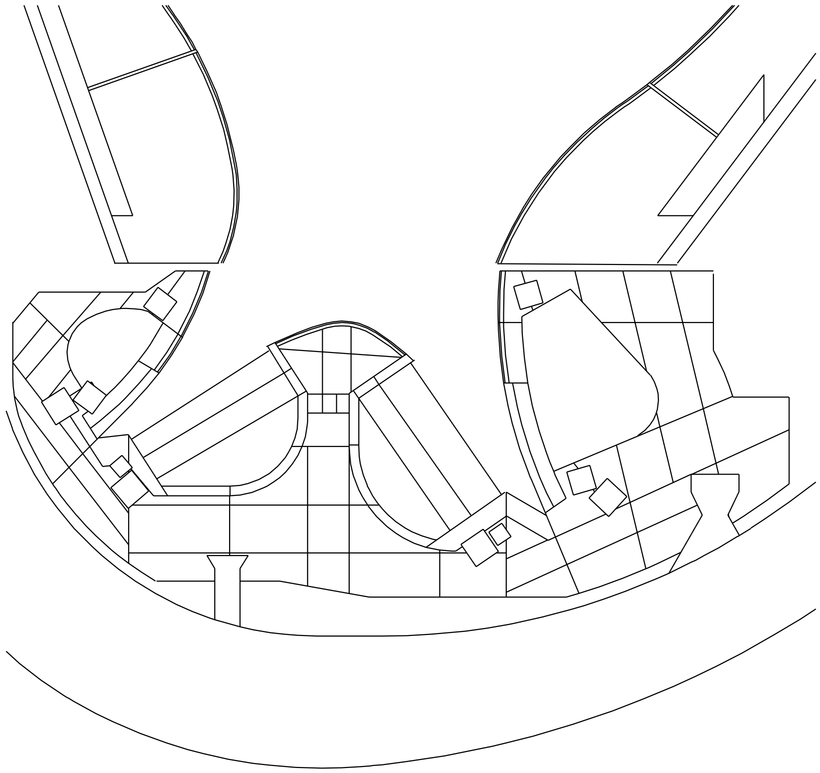

Fig. 5. Vertical cross section of divertor cassette in the 3-D model.

4. Multigroup Working Libraries Based on FENDL

A new processed MATXS library based on the international fusion evaluated nuclear data library (FENDL-1) has been provided by R.E. MacFarlane of Los Alamos National Laboratory. The library has 175 neutron - 42 gamma energy groups and includes gas production cross sections and radionuclide production cross sections. An algorithm for TRANSX was also provided to combine the radionuclide production cross sections with decay information to determine the decay heat contribution. The beta decay energy is assumed to be deposited locally and is added to the neutron kerma while the gamma production cross sections are modified to include the produced decay gammas thus allowing them to be transported before depositing their energy. This is a better treatment for decay gammas than assuming that all energy is deposited locally. We used the TRANSX [6] code to generate an updated working multigroup cross section library using the new processed MATXS multigroup library and the algorithm for inclusion of decay heat. This library includes nuclear data for 39 elements and isotopes required for ITER neutronics calculations. The library includes all nuclear responses of interest for the ITER design. Because of the large memory space needed for two-dimensional calculations, we generated a 46 neutron- 21 gamma group library by collapsing the large library using the standard VITAMIN-E weight function.

The two libraries were used to perform calculations for the FENDL calculational benchmark and the results were compared to those from the previous libraries. In general, good agreement was found between the gas production results from the recently processed FENDL multigroup library in which total gas production is included and from the previously processed library where we calculated the total gas production by adding the partial cross sections. The only exception is in the helium production in Be where the difference is a factor of 37. Further examination of partial reactions revealed that the contribution from (n,2n) reaction in Be that produces 2 alphas was not included in the total He production cross section in the new library. The effect on nuclear heating of the decay energy associated with short lived ($T_{1/2}$ < 1 day) radionuclides in the kerma factor is <7%. The new processed FENDL library includes decay energy for elements up to Cu only. Decay heat is not included yet for important elements such as Mo, Ni, Zr, Nb, Sn, W, and Pb.

5. Updating Activation Code and Libraries

Part of this task was aimed at modifying the activation code and its associated data libraries to allow for improved activation analysis. We expanded the DKR-PULSAR1.0 [7] code capabilities to allow for 3-D activation calculations. The activation cross section library was updated to include the latest cross section data from FENDL1.0. The original FENDL1.0 175 group neutron activation cross section data were collapsed to the 46 neutron group structure used by DKR-PULSAR1.0 using the VITAMIN-E weight function. The new cross section library contains data for 36 neutron reaction types and 8 decay types. The new library contains data for nuclides with Z < 85. We updated the DKR-PULSAR1.0 gamma source data according to the latest ENDF/B-VI values. The gamma source data are in a 21 gamma group structure. The library contains data for 1788 nuclides.

6. Building Activation Analysis

Activation calculations have been performed under this task agreement in support of the ITER building design task D325-2, subtask 01, Three-Dimensional Calculations of Building Dose Rate Profiles. The tokamak pit, pit access galleries, surrounding tokamak building spaces, and dirt were modeled simultaneously. The problem was modeled in a two-dimensional, r and z model using 116,921 mesh points. Radioactivity calculations were performed using the DKR-PULSAR1.0 code with FENDL1.0 activation cross section library. The gamma source from radioactive nuclide decay was determined for all mesh points at shutdown, 1 day following shutdown, 1 week following shutdown and 1 month following shutdown. The decay gamma source was provided to UCLA for dose calculations under the Task D325. The building dose map showed that special attention should be given to the NBI hall and divertor hall. Using the new implemented features in the DKR-PULSAR1.0 code package, we were able to perform pathway analysis to identify major contributors to the dose. We concluded that plugging the horizontal port immediately after shutdown will only drop the dose inside the NBI hall by about a factor of 2. On the other hand, the dose inside the divertor hall is within a factor of 3 ~ 4 of the desired level within a week following shutdown. Detailed results will be documented in the final report of task 325.

8. Summary and Conclusions

The Interim ITER Design has been modeled for 3-D neutronics calculations. The detailed 3-D divertor cassette model has been integrated with the general ITER model which includes detailed modeling of the first wall, blanket with associated coolant manifolds and back plates, VV, TF coils, central solenoid, and PF coils. All toroidal and poloidal gaps between adjacent blanket modules are included. The major vacuum vessel penetrations are included in the model. The neutronics parameters have been calculated in the different components of the divertor cassette. These parameters included nuclear heating, atomic displacement and helium production.

Radiation damage to parts of the vacuum vessel in the divertor region have been quantified to assess the feasibility of rewelding. The peak helium production value of about 0.5 He appm/FPY indicates that rewelding of parts of the VV behind the pumping ducts at the bottom of cassettes might be feasible. The peak magnet radiation effects have been calculated in segments of the TF coils in the divertor region. The radiation effects are higher at the side surface due to the effect of streaming. The calculated radiation effects are much lower than the radiation limits considered in ITER. The total nuclear heating in the parts of the 20 TF coils in the divertor region is 2.08 kW with 1.58 kW contributed by the parts adjacent to the divertor port. It is essential to determine the additional heating in the other parts of the coils and add them to the contribution from the divertor region to determine whether the total heating limit of 17 kW can be satisfied.

Modification of the 3-D model to include more details and design changes in the divertor cassette based on the ITER Detailed Design has started. Our effort concentrated on implementing the changes in the divertor cassette design that have been nearly fully developed. Separate regions are included to represent the mechanical attachments and coolant pipe connections for the dome, vertical targets, and wings. The layered configurations of the dome PFC and vertical targets were modeled accurately with the front tungsten layer modeled separately to properly account for self-shielding of the giant resonance at 20 eV that produces W-187. We will start implementing modifications in the blanket design when the design becomes fully developed.

Updated working multigroup cross section libraries with two different group structures have been generated based on the new processed FENDL-1 multigroup library. The libraries include gas production cross sections and decay energy. The beta decay energy is assumed to be deposited locally and is added to the neutron kerma while the gamma production cross sections are modified to include the produced decay gamma thus allowing them to be transported before depositing their energy. This is a better treatment for decay gamma than assuming that all energy is deposited locally.

The activation code DKR-PULSAR1.0 and its associated data libraries have been modified to allow for improved activation analysis. We expanded the DKR-PULSAR1.0 code capabilities to allow for 3-D activation calculations. The activation cross section library was updated to include the latest cross section data from FENDL1.0. We updated the DKR-PULSAR1.0 gamma source data according to the latest ENDF/B-VI values. Activation calculations have been performed under this task agreement in support for the ITER building dose calculation. The gamma source from radioactive nuclide decay was determined for all mesh points after shutdown for dose calculations.

References

[1] Technical Basis for the ITER Interim Design Report, Cost Review and Safety Analysis, ITER EDA Documentation Series, No. 7, International Atomic Energy Agency, Vienna, April 1996.

[2] J. Briesmeister, Ed., "MCNP, A General Monte Carlo N-Particle Transport Code, Version 4A," LA-12625-M, (1993).

[3] R. MacFarlane, "FENDL/MC-1.0, Library of Continuous Energy Cross Sections in ACE Format for MCNP-4A," Summary Documentation by A. Pashchenko, H. Wienke and S. Ganesan, Report IAEA-NDS-169, Rev. 3, International Atomic Energy Agency (Nov. 1995).

[4] ITER General Design Requirements, International Thermonuclear Experimental Reactor, 22 March 1996.

[5] ITER Conceptual Design Report, ITER Documentation Series no. 18, IAEA, Vienna, 1991.

[6] R. MacFarlane, "TRANSX 2: A Code for Interfacing MATX Cross Section Libraries to Nuclear Transport Codes," Los Alamos National Laboratory Report, LA-12312-MS (July 1992).

[7] D. Henderson et al., "DKR-Pulsar: A Radioactivity Calculation Code that Includes Pulsed/Intermittent Operation," to be published.